B physics at ATLAS

Lukáš Novotný

16th June 2022

Seen previously

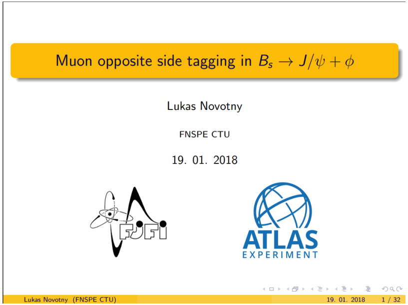

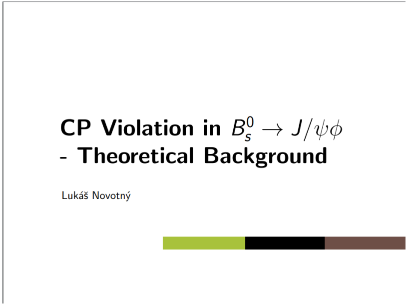

Content

B Physics Facilities

- B physics has been and is hot topic
- Helps understanding of elementary particles and their interactions
- Good channel for New Physics discoveries
- Important results in history
  - 1977: $\Upsilon(1S)$ at Fermilab (b-quark evidence)
  - 1983: B meson reconstructed at CLEO (B_d)
  - 1986: B_d mixing observed at ARGUS
  - 1900-2007 boom of B-physics results (next slide)
  - 2007-now: Precision measurements by LHC experiments ($B^0 \to \mu\mu$ discovery)
  - 2019-now: Belle-II results

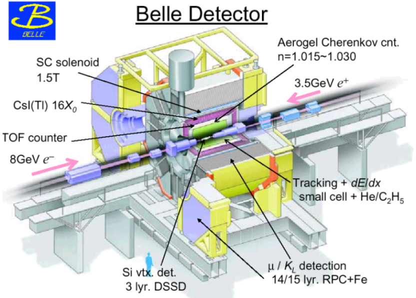

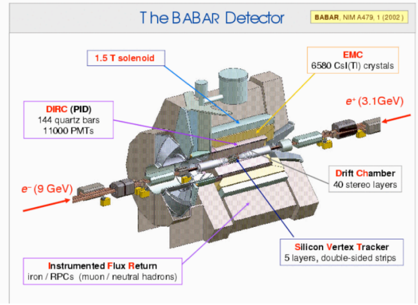

B Physics Facilities

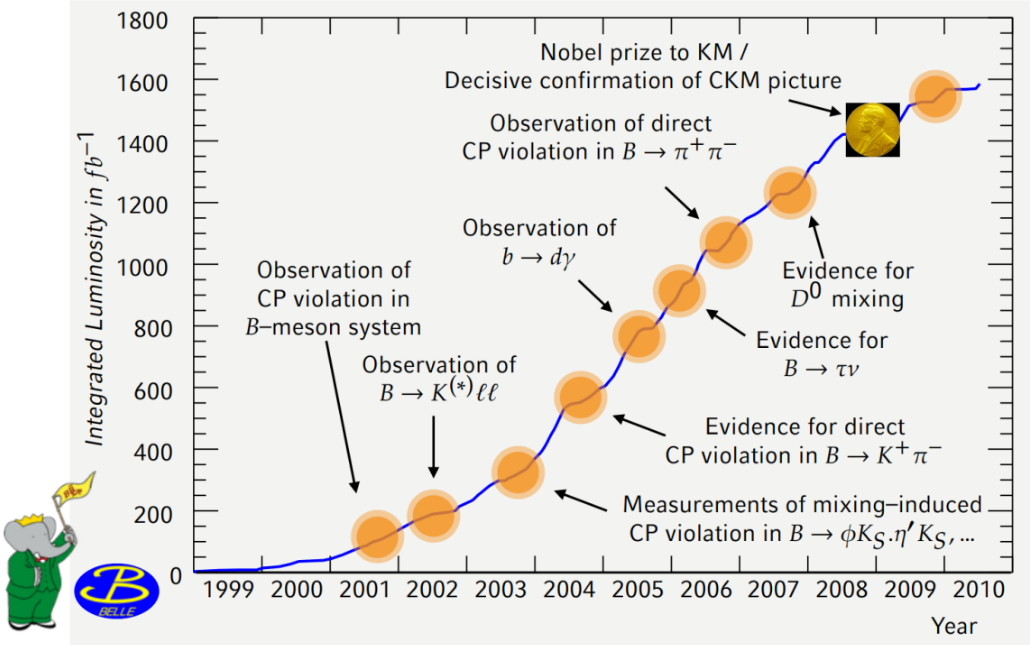

B-physics at LHC

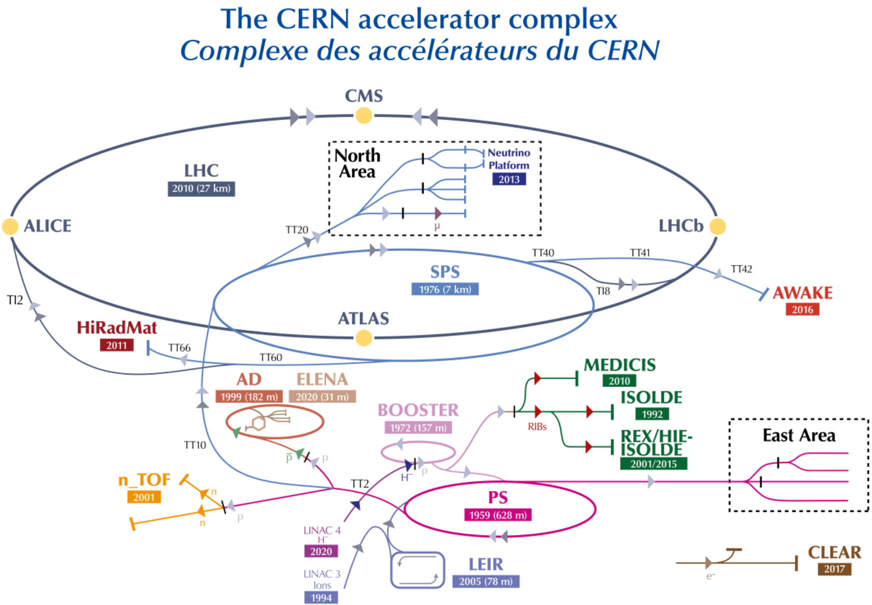
The CERN accelerator complex
Complexe des accélérateurs du CERN
CMS
North Area
Neutrino Platform
2013
LHC
2010 (27 km)
ALICE
LHCb
TT20
TT40
TT41
TT42
SPS
1976 (7 km)
TI8
AWAKE
2016
TI2
ATLAS
HiRadMat
2011
TT66
TT60
AD
1999 (182 m)
ELENA
2020 (31 m)
BOOSTER
1972 (157 m)
MEDICIS
2010
ISOLDE
1992
RIBs
REX/HIE-ISOLDE
2001/2015
East Area
TT10
n_TOF
2001
TT2
PS
1959 (628 m)
LINAC 4
H⁻
2020
LINAC 3
Ions
1994
LEIR
2005 (78 m)
CLEAR
2017

LHC

- 27 km ring, proton-proton collider, energies: $\sqrt{s}$ =7, 8, 13, 13.8 TeV
- Collision rate: 40MHz
- 8 interaction points (IP)
- 4 large experiments (ALICE, ATLAS, CMS, LHCb)
- CMS and ATLAS: general purpose detectors
- LHCb: dedicated for B physics
- Totally: 29 fb^{-1} in Run1 and 185 fb^{-1} in Run2 of high energy *pp* collisions

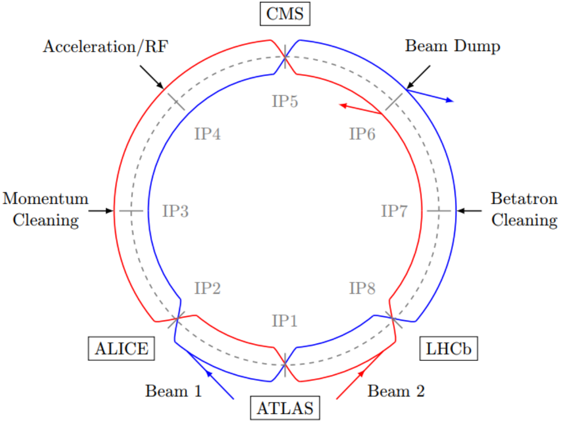

LHC fill pattern

- Injection: Magnet current increased, bunches injected from SPS
- Ramp: Beams accelerated to collision energy
- Squeeze and adjust: Beam size at the IP is reduced (squeeze) and prepared for the collision (adjust)
- Stable beams: Colliding the beams at the IPs, small adjustments, 50% of the time LHC at stable beams
- Dump and ramp down: Beams extracted from the LHC and safely dumped. Magnetic fields are ramp down

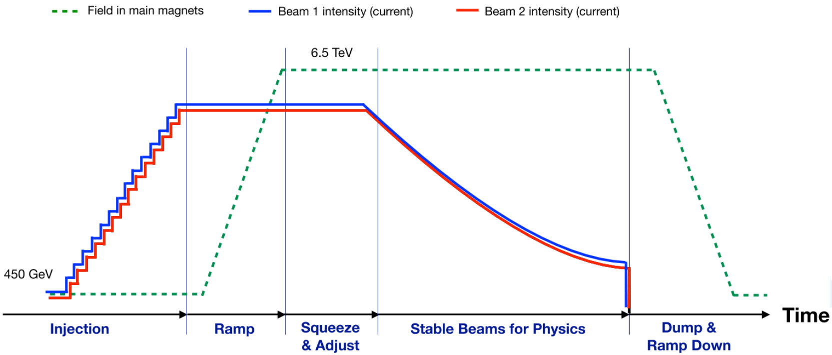

The ATLAS Collaboration

Argentina
Armenia
Australia
Austria
Azerbaijan
Belarus
Brazil
Canada
Chile
China
Colombia
Czech Republic
Denmark
France
Georgia
Germany
Greece
Israel
Italy
Japan
Mongolia
Morocco
Netherlands
Norway
Palestine
Philippines
Poland
Portugal
Romania
Russia
Serbia
Slovakia
Slovenia
South Africa
Spain
Sweden
Switzerland
Taiwan
Turkey
UAE
UK
USA
CERN
JINR

ATLAS Collaboration

181 institutions (245 institutes) from 42 countries

The ATLAS Experiment

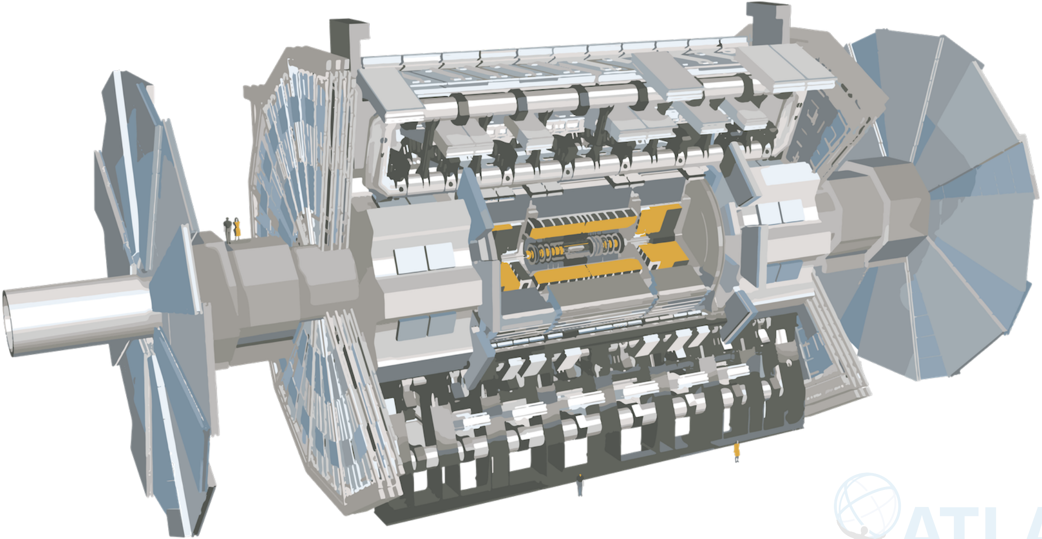

The ATLAS Detector

Muon Spectrometer ($|\eta|<2.7$) :
air-core toroids with gas-based muon chambers
Muon trigger and measurement with
momentum resolution < 10% up to E_μ ~ 1 TeV

Length : ~ 46 m
Radius : ~ 12 m
Weight : ~ 7000 tons
~10^8 electronic channels
3000 km of cables

3-level trigger
reducing the rate
from 40 MHz to
~200 Hz

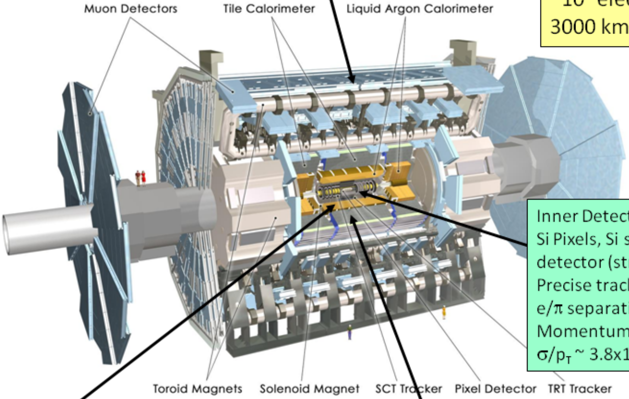

Inner Detector ($|\eta|<2.5$, B=2T):
Si Pixels, Si strips, Transition Radiation
detector (straws)
Precise tracking and vertexing,
e/π separation
Momentum resolution:
$\sigma/p_T \sim 3.8\text{x}10^{-4}\ p_T\,(\text{GeV}) \oplus 0.015$

EM calorimeter: Pb-LAr Accordion
e/γ trigger, identification and measurement
E-resolution: $\sigma/E \sim 10\%/\sqrt{E}$

HAD calorimetry ($|\eta|<5$): segmentation, hermeticity
Fe/scintillator Tiles (central), Cu/W-LAr (fwd)
Trigger and measurement of jets and missing E_T
E-resolution: $\sigma/E \sim 50\%/\sqrt{E} \oplus 0.03$

ATLAS Trigger System

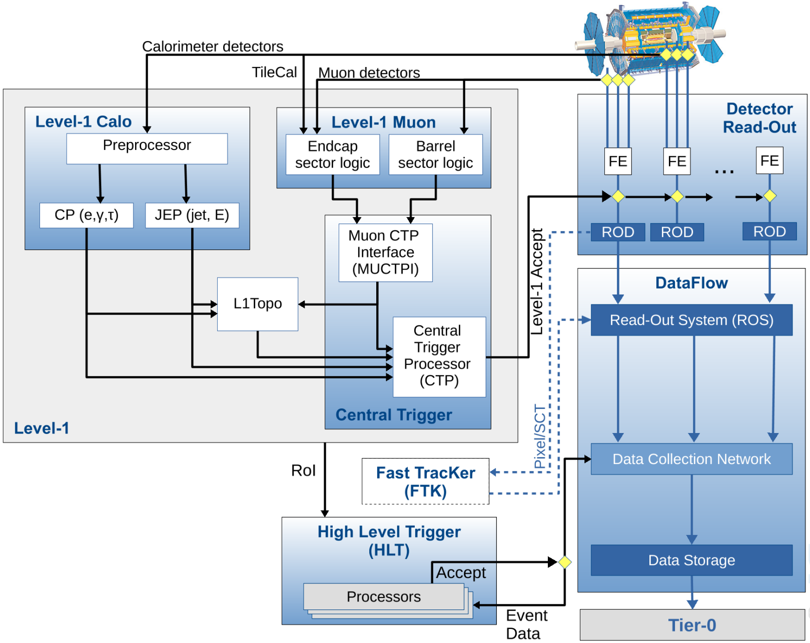

ATLAS Trigger System

ATLAS TDAQ system

- Online processing, selecting and storing events of interest for offline analysis
- Two stage trigger system: **L1** and **HLT**
- 40 MHz (bunch crossing) $\rightarrow$ 100 kHz (L1) $\rightarrow$ 1.2 kHz (HLT, 1.2 GB/s)

L1 Trigger

- Hardware-based system
- custom electronics to trigger on reduced-granularity information from the calorimeter (L1Calo) and muon detectors (L1Muon)
- **L1Calo**
  - Cluster Processor (CP): identifies **electron**, **photon**, and τ-**lepton**
  - Jet/Energy-sum Processor (JEP): identifies **jet candidates** and produces global sums of total and missing transverse energy
- **L1Muon**
  - uses hits from the RPCs (in the barrel) and TGCs (in the endcaps)
  - determines the deviation of the hit pattern from that of a muon with infinite momentum

ATLAS Trigger System

L1 Trigger

- Central Trigger Processor (CTP)
  - L1 trigger decision formed here
  - Take as an input: L1Calo trigger, L1Muon trigger and L1Topo (FPGA, algorithms looking for physics - e.g. $B^0 \to e^{\pm}\mu^{\pm}$
  - Trigger signals from several detector subsystems (LUCID, ZDC)
  - Applies the dead time - limit of the L1 acceptance rate
- When event accepted by L1, Front-End (FE) detector electronics read out the event data from each detector
  - ReadOut Drivers (RODs): initial processing and formatting
  - ReadOut System (ROS): buffer the data

High-Level Trigger (HLT)

- Software-based
- largely based on the offline software Athena (itself is based on Gaudi, a framework for data processing for HEP experiments)
- Uses RoI from L1 as an input
- HLT determines the RoI on a hypothesis algorithm (identification algorithms and pile-up rejection methods)
- Not only one algorithm used $\to$ triggers (trigger menu)

- Data recorded at an average rate ~1.2 kHz
  - 200 Hz for B-physics and Light State (BLS)
  - 1 kHz for all other main physics data

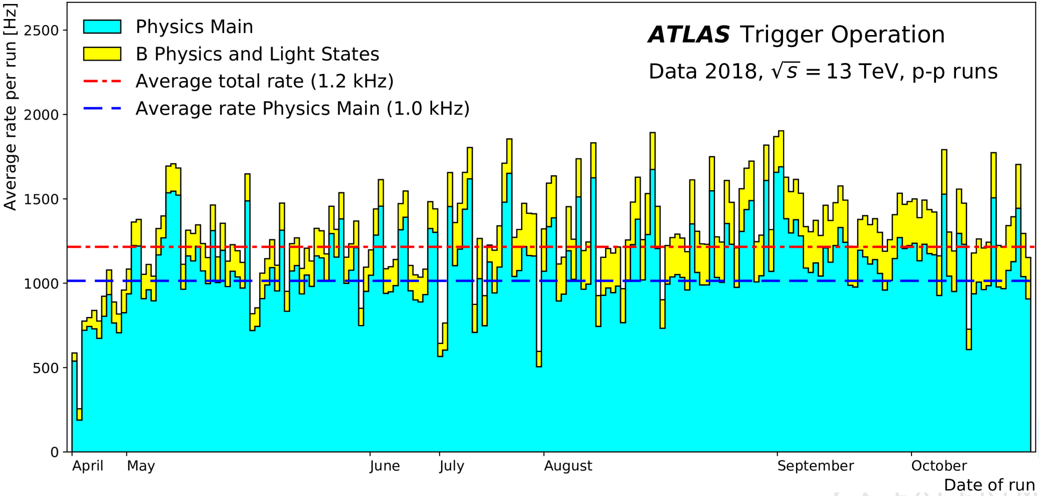

ATLAS B-physics Triggers

- At LHC, only 1% contains $b\bar{b}$ events
- Only 5% of triggers suitable for BLS need to be highly selective
- Only BLS data kept separate for the offline reconstruction
- BLS trigger based on di-muon triggerat the L1 stage
  - 4 GeV + 4 GeV
  - 4 GeV + 6 GeV
  - 6 GeV + 6 GeV
- Single muon triggers (15 GeV at L1, 20 GeV at HLT)
- Without further requirements, too large rate would be obtained = large prescale factors (trigger rate is much larger than L1 or HLT trigger)
  - L1Topo used to reduce the di-muon trigger rates while retaining sensitivity

Trigger	**Unprescaled rate**	**Target rate**	**Total prescale**	**L1 prescale**	**HLT prescale**
HLT_mu15_L1MU10	100 Hz	20 Hz	5	5	1
HLT_mu10_L1MU10	200 Hz	20 Hz	10	5	2

ATLAS B-physics Triggers

- For example, L1Topo critical for $B_s \to \mu\mu$

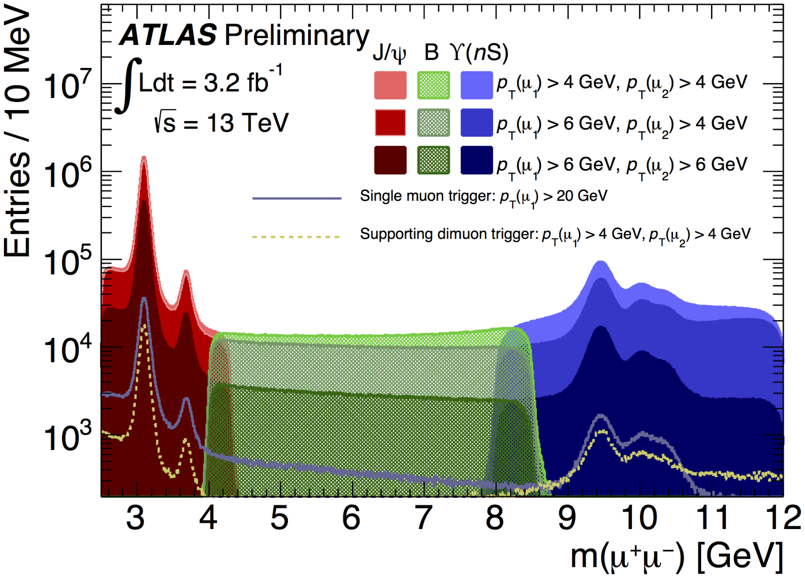

ATLAS B-physics Triggers

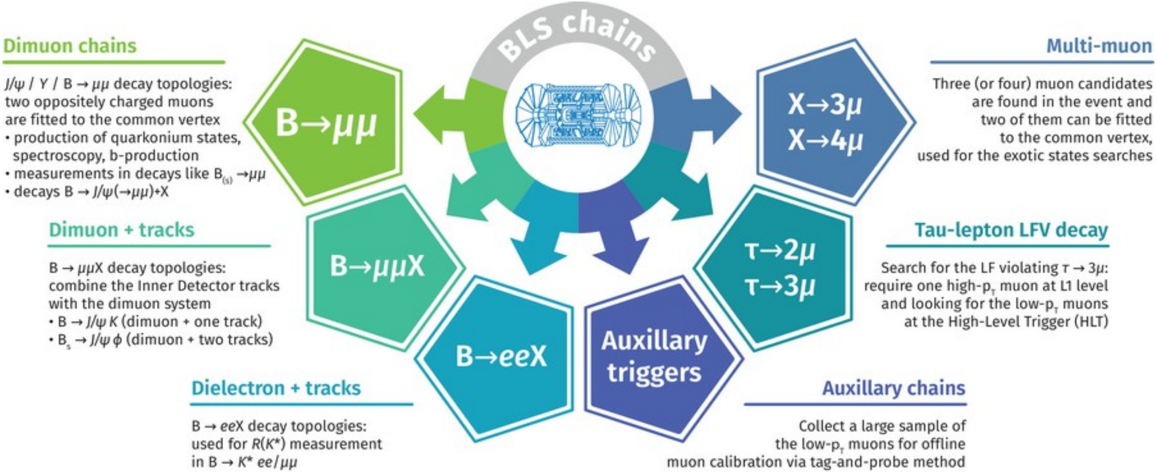

BLS activities, analyses

Structure of BLS analyses:

- Onia production and b cross section
  - Search for 4μ resonances at low masses
  - Extract gluon Transverse Momentum Dependent Parton Distribution functions (TMDs) in the proton using $J/\psi + \gamma$
  - Cross-section Measurement of Associated $J/\psi + W^+$ Production
  - Looking for the decay $W^+ \to J/\psi + D_s^+$
- Rare decays
  - Angular analysis of $B_d \to K^*(892)\mu^+\mu^-$
  - Search for $B_{(s)} \to \mu\mu$
  - Search for $\tau \to 3\mu$
  - $R(K^*)$ measurement
- Physics with $B \to J/\psi$
  - B^+ cross-section measurement
  - Searches for pentaquarks
  - CP violation in $B_s^0 \to J/\psi\phi$
  - B_d^0 and B^+ lifetime measurement
  - Search for $Z_c(4200)$ in B^0ßJ/\psi K\pi$ decays
  - Study of $B_c^+ \to D_s^{(*)+}$
  - B_c/B^+ production ratio measurement

BLS activities, analyses

Structure of BLS analyses:

- Onia production and b cross section
  - Search for 4μ resonances at low masses
  - Extract gluon Transverse Momentum Dependent Parton Distribution functions (TMDs) in the proton using $J/\psi + \gamma$
  - Cross-section Measurement of Associated $J/\psi + W^+$ Production
  - Looking for the decay $W^+ \to J/\psi + D_s^+$
- Rare decays
  - Angular analysis of $B_d \to K^*(892)\mu^+\mu^-$
  - **Search for $B_{(s)} \to \mu\mu$**
  - Search for $\tau \to 3\mu$
  - $R(K^*)$ measurement
- Physics with $B \to J/\psi$
  - B^+ cross-section measurement
  - Searches for pentaquarks
  - **CP violation in $B_s^0 \to J/\psi\phi$**
  - **B_d^0 and B^+ lifetime measurement**
  - Search for $Z_c(4200)$ in B^0ß$J/\psi K\pi$ decays
  - Study of $B_c^+ \to D_s^{(*)+}$
  - B_c/B^+ production ratio measurement

Measurement of the CP-violating phase ϕ_s in $B_s^0 \to J/\psi\phi$ decays in ATLAS at 13 TeV

CP Violation in $B_s^0 \to J/\psi\phi$

- In $B_s^0 \to J/\psi\phi$, CP violation appears due to interference between a direct decay and a decay with $B_s^0 - \bar{B}_s^0$ mixing
- CP violation measured via CP-violation phase ϕ_s
- ϕ_s predicted by SM and related to CKM matrix

$$\phi_s = 2\arg\left[\frac{V_{ts}V_{tb}^*}{V_{cs}V_{cb}^*}\right] = -0.03696^{+0.00072}_{-0.00082}\ \mathrm{rad}$$

- **Any violation** from this values would be hint for **New Physics (Beyond Standard Model physics)**

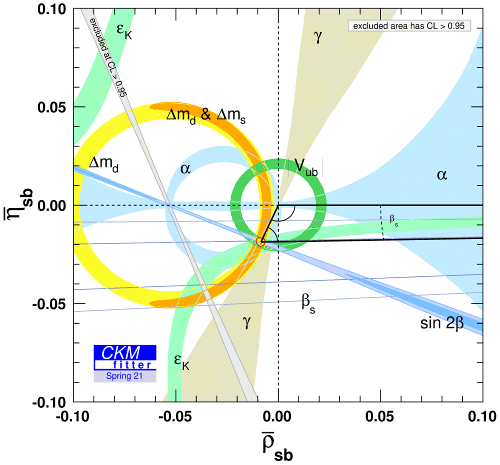

Motivation

***CP* violation measurement in $B_s^0 \to J/\psi\phi$** Eur. Phys. J. C 81 (2021) 342

- The other quantities in B_s^0 mixing are $\Delta m_s = |m_L - m_H|$, $\Delta\Gamma_s = \Gamma_s^L - \Gamma_s^H$ and $\Gamma_s = (\Gamma_s^L + \Gamma_s^H)/2$
  - $\Delta\Gamma_s$, Γ_s not as sensitive to New Physics, however the measurement is interesting to test the theory ($\Delta\Gamma_s = (0.091 \pm 0.013)\ \mathrm{ps}^{-1}$)
- Situation before LHC Run2:

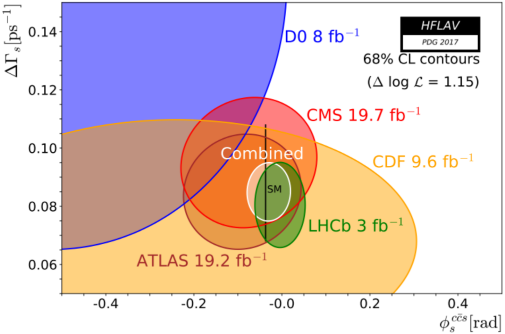

Eur. Phys. J. C 81 (2021) 226

- Similar measurements were previously performed at the LHC in Run1 and at the Tevatron by the CDF and D0 experiments

CP Violation and Lifetime Measurement: Angular Analysis

- $B_s^0 \to J/\psi\phi$ is a decay of pseudoscalar into a pair of vectors
- Final state: admixture of CP-odd (L = 1) and CP-even (L = 0, 2) states
- Contribution from non-resonant S-wave $B_s^0 \to J/\psi K^+K^-$ - CP-odd
- Distinguishable through time-dependent angular analysis
- differential decay rate depends on amplitudes A_0, $A_\perp$, $A_\parallel$, A_S (and interferences) and angles θ_T, ψ_T, ϕ_T

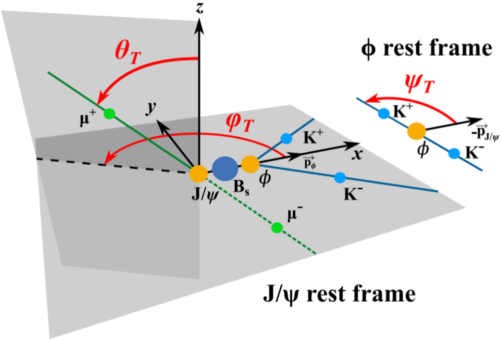

CP Violation and Lifetime Measurement: Parameters of Interest

- Unbinned maximum likelihood fit performedon the combined data samples extracting parameters of interest
  - CP-violating phase ϕ_s
  - The average decay width Γ_s and the decay width difference $\Delta\Gamma_s$
  - The *CP*-state amplitudes at $t = 0$: $|A_0(0)|^2$, $|A_\perp(0)|^2$, $|A_\parallel(0)|^2$, $|A_S(0)|^2$

$$|A_0(0)|^2 + |A_\perp(0)|^2 + |A_\parallel(0)|^2 = 1$$

  - The strong phases $\delta_\perp$, $\delta_\parallel$, $\delta_0 = 0$, δ_S
  - ATLAS sensitive to $\delta_\perp$, $\delta_\parallel$ and $\delta_S - \delta_\perp$
- No direct *CP* violation assumed
- $\Delta m_s = |m_L - m_H|$ value fixed to PDG: $\Delta m_s = 17.77\ \mathrm{ps}^{-1}$
- Opposite side tagging (OST) used to identify initial flavour of B_s^0

- Opposite side tagging (Tight muons, Electrons, Low-p_{T} muons and Jets),
  - Events tagged by the method with the highest statistical power

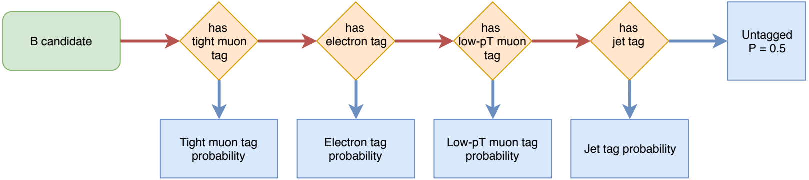

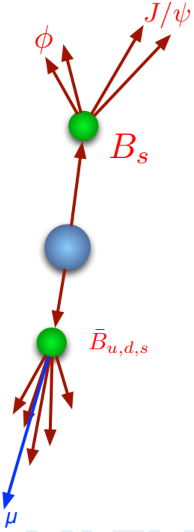

- Muon and Electron Tagging
  - $b \to l$ transitions are clean tagging method
  - $b \to c \to l$ and neutral B-meson oscillations dilute the tagging
  - Tracks in cone around lepton also included $\Rightarrow$ weighted sum of charges used
- Jet-Charge
  - information from tracks in b-tagged Jet, when no lepton is found
- Calibration using $B^{\pm} \to J\psi K^{\pm}$

CP Violation and Lifetime Measurement: Opposite Side Tagging

- Cone around OST lepton:

$$Q = \frac{\sum_i^{Ntracks} q^i (p_T^i)^\kappa}{\sum_i^{Ntracks} (p_T^i)^\kappa} \rightarrow P(Q|B^\pm)$$

- The probability to tag a B_s^0 meson as containing a $\bar{b}$-quark:

$$P(B|Q) = \frac{P(Q|B^+)}{P(Q|B^+) + P(Q|B^-)}$$

- Tagging performance quality described by:
  - **Efficiency ε:** Fraction of tagged events
  - **Dilution:** $D = (1 - 2\omega)$, where ω is the mistag probability
  - **Tagging Power:** $T = \varepsilon D^2$ figure of merit of tagger performance

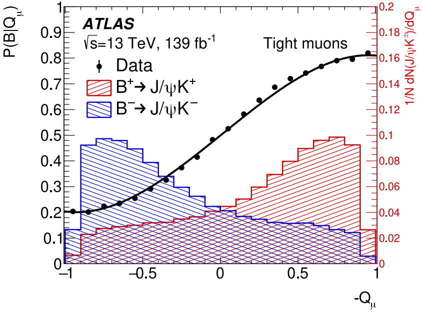

Tag method	ϵ_x [%]	D_x [%]	T_x [%]
Tight muon	4.50 ± 0.01	43.8 ± 0.2	0.862 ± 0.009
Electron	1.57 ± 0.01	41.8 ± 0.2	0.274 ± 0.004
Low-p_T muon	3.12 ± 0.01	29.9 ± 0.2	0.278 ± 0.006
Jet	12.04 ± 0.02	16.6 ± 0.1	0.334 ± 0.006
Total	21.23 ± 0.03	28.7 ± 0.1	1.75 ± 0.01

CP Violation and Lifetime Measurement: Fit Model

- Unbinned maximum likelihood fit:

tau weight — signal — peaking background — combinatorial background

$$\mathcal{L} = \sum_{i=1}^{N} \{ w_i \cdot \ln(f_s \mathcal{F}_s + f_s \cdot f_{B_d^0} \mathcal{F}_{B_d^0} + f_s f_{\Lambda_b} \mathcal{F}_{\Lambda_b} + (1 - f_s)(1 + f_{B_d^0} + f_{\Lambda_b}) \mathcal{F}_{\mathrm{bkg}})\}$$

- Base observables: mass m, lifetime t, angles $\Omega(\psi_T, \phi_T, \theta_T)$
- Conditional observables per-candidate: mass and lifetime resolution (σ_m, σ_t), candidate p_{T}, tagging probability and method
- Likelihood corrected to tau weight - trigger efficiencies
- Contributions from: $B_d \to J/\psi K^{*0}$, $B_d \to J/\psi K\pi$ and $\Lambda_b \to J/\psi Kp$ misidentified as B_s^0 candidates
  - Efficiencies and acceptance from MC
  - BR from PDG
  - Fragmentation fractions from other measurements

- Extensive systematic study was performed
- Here is the list of the major contributions to the total systematics:
  - **Flavour tagging:** calibration, $B_s^0 - B^{\pm}$ MC difference and dependencies on the pile-up distribution
  - **Fit bias:** fit stability is validated by the pseudo-experiments with default fit results
  - **Background angles model:** varying the bin boundaries, invariant mass window and sideband definition
  - **Best candidate selection:** statistically equivalent sample is created where all candidates in the event are retained
  - **Angular acceptance method:** different acceptance functions are calculated using different numbers of p_{T} bins as well as different widths and central values of the bins

CP Violation and Lifetime Measurement: Results

- Results - two solutions observed for strong phases
  - Well separated local maxima in the likelihood
    - Interesting parameters are almost insensitive to strong phase ambiguity

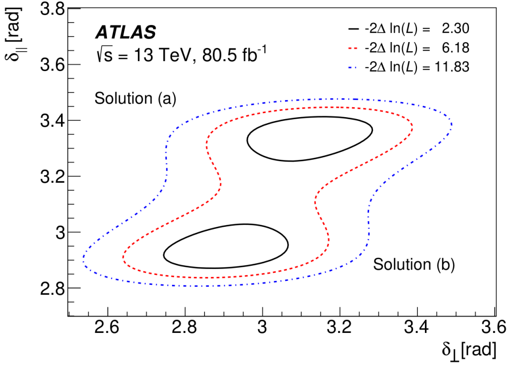

Parameter	Value	Statistical uncertainty	Systematic uncertainty
ϕ_s [rad]	-0.081	0.041	0.022
$\Delta\Gamma_s$ [ps^{-1}]	0.0607	0.0047	0.0043
Γ_s [ps^{-1}]	0.6687	0.0015	0.0022
$\lvert A_{\parallel}(0)\rvert^2$	0.2213	0.0019	0.0023
$\lvert A_0(0)\rvert^2$	0.5131	0.0013	0.0038
$\lvert A_S(0)\rvert^2$	0.0321	0.0033	0.0046
$\delta_{\perp} - \delta_S$ [rad]	-0.25	0.05	0.04
Solution (a)			
$\delta_{\perp}$ [rad]	3.12	0.11	0.06
$\delta_{\parallel}$ [rad]	3.35	0.05	0.09
Solution (b)			
$\delta_{\perp}$ [rad]	2.91	0.11	0.06
$\delta_{\parallel}$ [rad]	2.94	0.05	0.09

CP Violation and Lifetime Measurement: Results

- Projections of mass $m(J/\psi\phi)$, lifetime t and three transversity angles $\Omega(\psi_T, \phi_T, \theta_T)$
- Combinatorial background for angular distribution use Legendre polynomials from sidebands

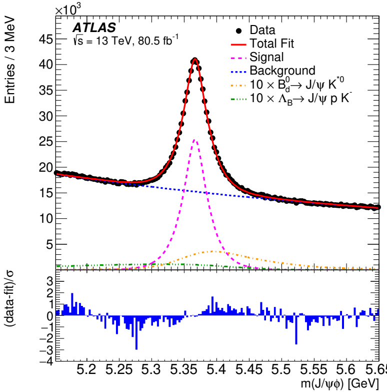

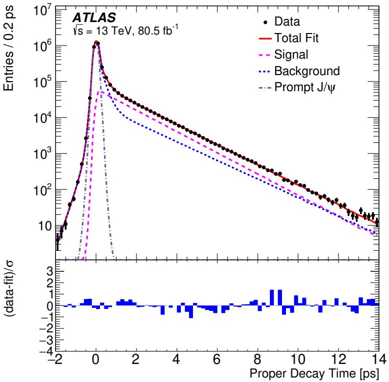

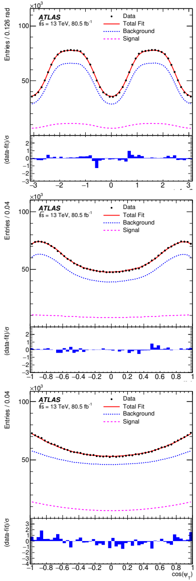

CP Violation Measurement: Results

- Used 80.5 fb^{-1} of 2015-17 data from *pp* collisions collected by the ATLAS detector
- Combined with Run 1 results: 4.9 fb^{-1} (7 TeV, *pp* 2011) and 14.3 fb^{-1} (8 TeV, *pp* 2012)

$$\phi_s = -87 \pm 36(\text{stat.}) \pm 21(\text{syst.})\ \text{mrad}$$

$$\Delta\Gamma_s = 65.7 \pm 4.3(\text{stat.}) \pm 3.7(\text{syst.})\ \text{ns}^{-1}$$

$$\Gamma_s = 670.3 \pm 1.4(\text{stat.}) \pm 1.8(\text{syst.})\ \text{ns}^{-1}$$

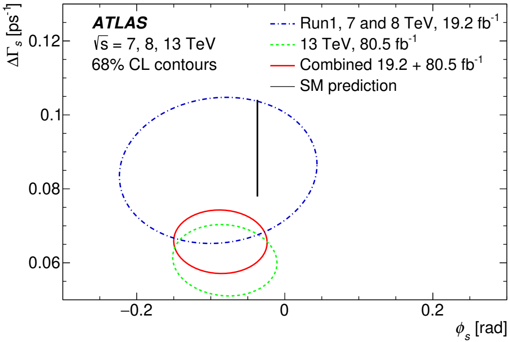

CP Violation Measurement: HL-LHC Prospects

ATL-PHYS-PUB-2018-041

- Updated tracking (ITk): proper decay time resolution improved by 21% w.r.t. Run 2
- Three trigger scenarios:
  - 2MU10: $18 \times N_{\mathrm{Run1}}$
  - MU6_MU10: $60 \times N_{\mathrm{Run1}}$
  - 2MU6: $100 \times N_{\mathrm{Run1}}$
- N_{sig} and σ_t scale with statistics, tag power not scaled
- Expected improvements w.r.t. Run 1
  - ϕ_s stat. uncertainty: better by $\sim 9\times$ to $20\times$
  - $\Delta\Gamma$ stat. uncertainty: better by $\sim 4\times$ to $10\times$
- LHC Run2 results not included in this study

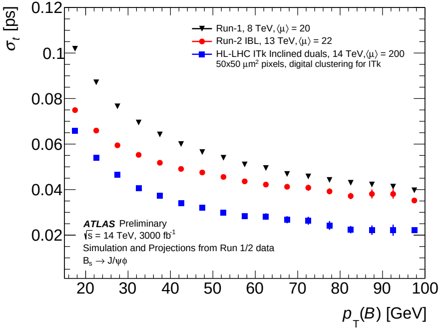

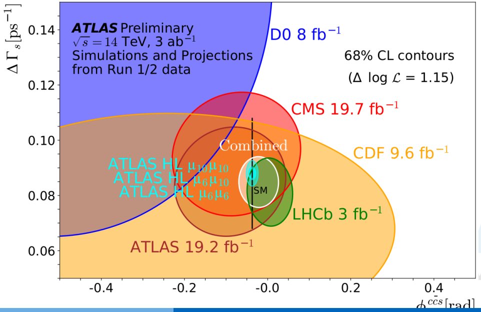

B_d^0 lifetime measurement

B_d^0 lifetime measurement

- Lifetime of B_s^0 from CP violation measurent shows tension with other experiments results
- Complementary measurement of B-meson lifetimes needed
- B_d^0 is a mixture of B_L^0 and B_H^0
  - The effective lifetime is measured:

$$\tau_{eff} = \frac{1}{\Gamma}\frac{1}{1-y^2}\left(\frac{1+Ay+y^2}{1+Ay}\right)$$

  - $\Delta\Gamma = \Gamma_L - \Gamma_H$, $y = \Delta\Gamma/(2\Gamma)$ and A depends on decay rate of the members of the system to final state
- Fractions of lifetime can be predicted by Heavy Quark Expansion (HQE) framework
  - decay rate of a hadron containing a heavy quark (b,c) can be expressed in a power series of the inverse of the heavy quark mass

$$\tau(B^+)/\tau(B_d^0) = 1.082^{+0.022}_{-0.026}$$

$$\tau(B_d^0)/\tau(B_d^0) = 1.0007 \pm 0.0025$$

B_d^0 lifetime measurement

- Psedo-proper lifetime used in the analysis:

$$\tau = \frac{L}{\beta\gamma c} \quad \rightarrow \quad \tau = \frac{L_{xy} m_{B_d}}{P_{\mathrm{T}}(B_d)}$$

- Unbinned mass-lifetime fit performed, lifetime per-candidate-error used (Punzi)

$$L = \prod_{i=1}^{N} (f_{sig} \mathcal{M}_{sig} T_{sig} + f_{peak} \mathcal{M}_{peak} T_{peak} + (1 - f_{sig} - f_{peak}) \mathcal{M}_{bkg} T_{bkg})$$

- **Signal:** mass described by two Johnson functions, lifetime by single exponential convoluted by resolution function (3 gaussian)
- **Background:** mass described by two exponential functions, lifetime by three exponential convoluted by resolution function
- **Peaking background:** $B^{\pm} \rightarrow J/\psi K^{\pm}$, $B_s^0 \rightarrow J/\psi K^+ K^-$ and $B_d \rightarrow J/\psi \rho(\pi^+ \pi^-)$

B_d^0 lifetime measurement

- Peaking ackground missing now - WIP

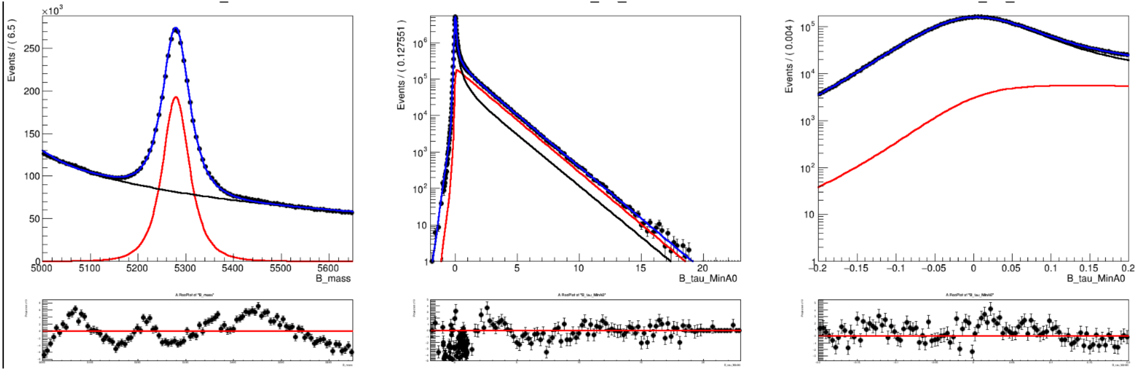

B_d^0 lifetime measurement

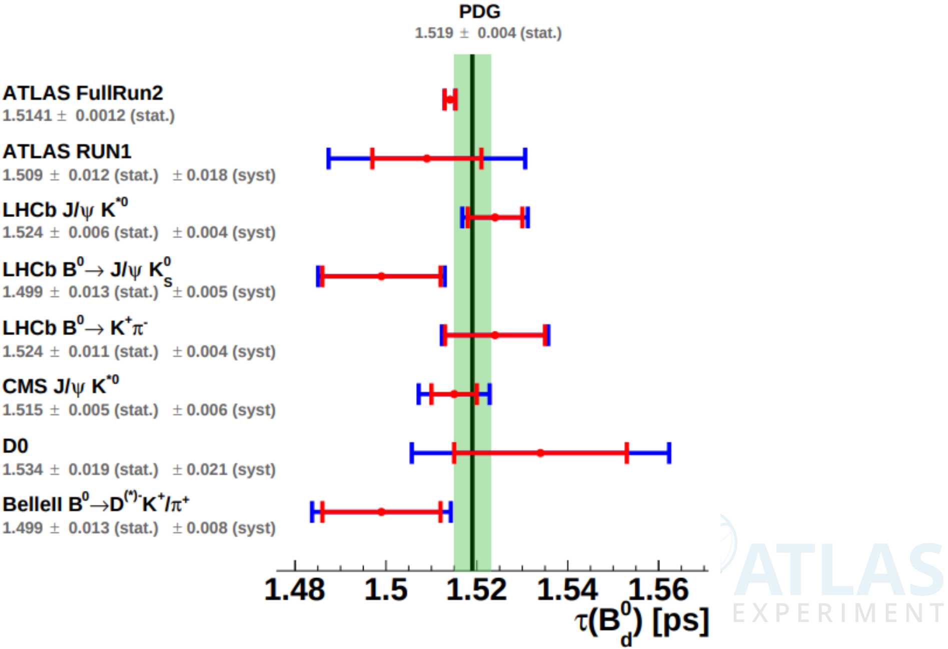

Search for $B^0_{(s)} \to \mu\mu$

$B^0_{(s)} \to \mu\mu$

- FCNC processes **highly supressed in SM**, significant deviations predicted by theories beyond SM
- $B^0_s \to \mu\mu$ and $B^0 \to \mu\mu$ highly sensitive to New Physics
- SM predictions: $\mathcal{B}\left(B^0_s \to \mu\mu\right) = (3.66 \pm 0.14) \cdot 10^{-9}$ and $\mathcal{B}\left(B^0 \to \mu\mu\right) = (1.03 \pm 0.05) \cdot 10^{-10}$
- Branching fractions are measured relative to the reference decay mode $B^\pm \to \mathrm{J}/\psi K^\pm$:

$$\mathcal{B}\left(B^0_{(s)} \to \mu\mu\right) = N_{d(s)} \frac{\mathcal{B}\left(B^\pm \to \mathrm{J}/\psi K^\pm\right) \times \mathcal{B}\left(\mathrm{J}/\psi \to \mu\mu\right)}{N_{\mathrm{J}/\psi K^\pm} \frac{\varepsilon_{\mu\mu}}{\varepsilon_{\mathrm{J}/\psi K^\pm}}} \frac{f_u}{f_{d(s)}}$$

  - Branching ratios known from PDG, $f_u/f_{d(s)}$ from HFLAV
  - Relative reconstruction efficiencies estimated from MC (corrected for data-MC differences): $\varepsilon_{\mu\mu}/\varepsilon_{\mathrm{J}/\psi K^\pm} = 0.1176 \pm 0.0009(\mathrm{stat.}) \pm 0.0047(\mathrm{syst.})$
  - Yields $N_{d(s)}$ and $N_{\mathrm{J}/\psi K^\pm}$ exctracted from unbinned ML fit
- $B^0_s \to \mathrm{J}/\psi\phi$ used as control channel

$B^0_{(s)} \to \mu\mu$

- Partially reconstructed *b*-hadrons
  - one or more of the final-state particles (X) in a *b*-hadron decay is not reconstructed
  - Mostly in the low di-muon mass region
- Peaking backgrounds
  - $B^0_{(s)} \to hh'$ decays, both hadrons misreconstructed as muons
  - Simulated and fixed in the mass fit
- Continuum background
  - Muons originating from uncorrelated hadron decays
  - Reduced by BDT (15 variables)

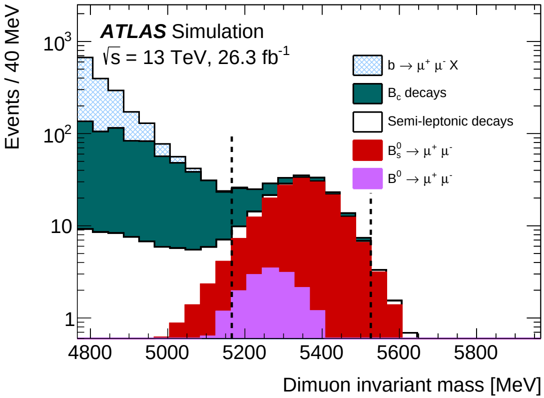

$B^0_{(s)} \to \mu\mu$

- BDT with 15 variables used (kinematics, isolation)
- BDT output validated on reference and control channels
- Signal region divided into four BDT bins
- B^0_s and B^0 yields extracted from simultaneous unbinned ML fit

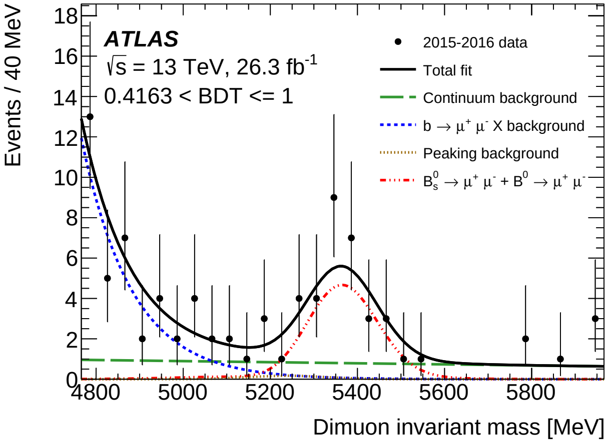

$B^0_{(s)} \to \mu\mu$

- Results combined with ATLAS Run1:

$$\mathcal{B}\left(B^0_s \to \mu\mu\right) = \left(2.8^{+0.8}_{-0.7}\right) \cdot 10^{-9}$$

$$\mathcal{B}\left(B^0 \to \mu\mu\right) < 2.1 \cdot 10^{-10} \text{at } 95\% \text{ CL}$$

- Combined measurement compatible with SM at 2.4σ
- Statistic uncertainties dominate
- 2.1σ compatibility of LHC combination and SM

$B^0_{(s)} \to \mu\mu$

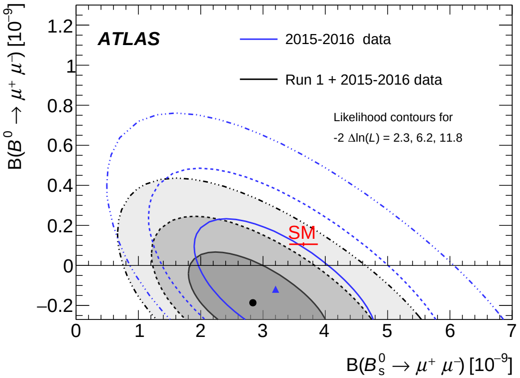

ATLAS
2015-2016 data
Run 1 + 2015-2016 data
Likelihood contours for
-2 Δln(L) = 2.3, 6.2, 11.8
SM
B(B⁰ → μ⁺ μ⁻) [10⁻⁹]
B(B⁰ₛ → μ⁺ μ⁻) [10⁻⁹]

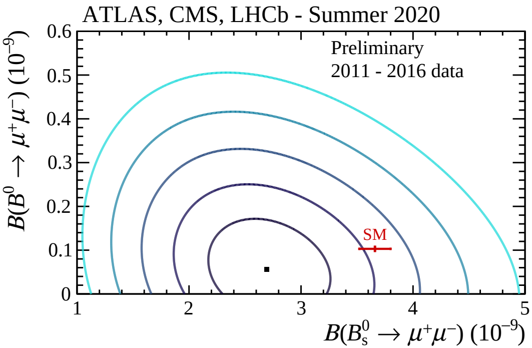

ATLAS, CMS, LHCb - Summer 2020
Preliminary
2011 - 2016 data
SM
B(B⁰ → μ⁺μ⁻) (10⁻⁹)
B(B⁰ₛ → μ⁺μ⁻) (10⁻⁹)

Summary

- LHC accelerating ring introduced
- ATLAS has rich program, B-physics play important role
- Many B-physics analyses provide very interesting results

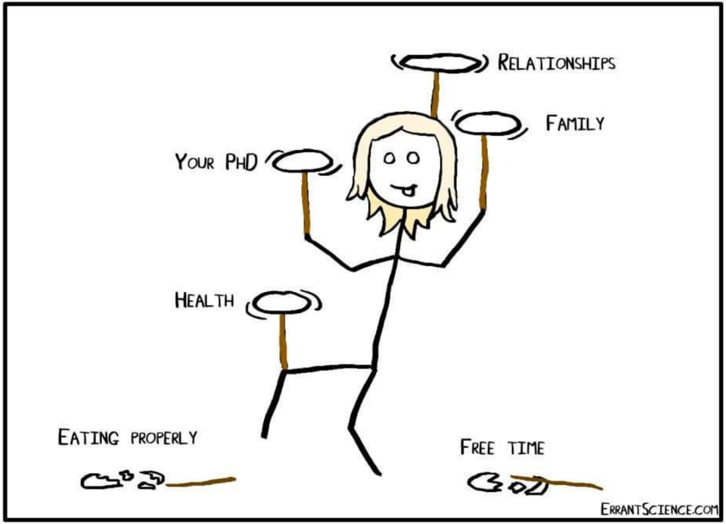

Back-up Slides

Λ_b Lifetime Measurement in ATLAS Run1

- Used 4.9 fb^{-1} of 2011 data from *pp* collisions collected by the ATLAS detector at energies $\sqrt{s}$ =7 TeV
- Decay channel $\Lambda_b \to J/\psi(\mu^+\mu^-)\Lambda^0(p\pi^-)$ used
- Mass-lifetime unbinned maximum likelihood fit used

$$\tau_{\Lambda_b} = 1.449 \pm 0.036(\text{stat.}) \pm 0.017(\text{syst.})\ \text{ps}$$

- $B_d \to J/\psi K_S$ lifetime measured as a cross-check

$$\tau_{\Lambda_b} = 1.509 \pm 0.012(\text{stat.}) \pm 0.018(\text{syst.})\ \text{ps}$$

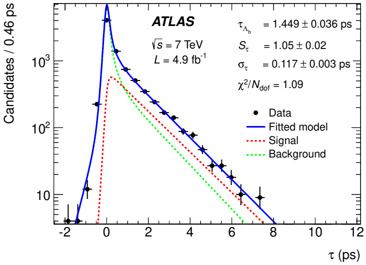

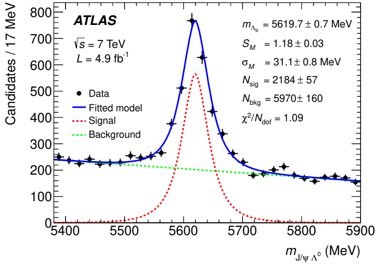

$\Delta\Gamma_d/\Gamma_d$ of the $B^0 - \overline{B}^0$ system in ATLAS Run1

- Used 25.2 fb^{-1} of 2011-12 data from pp collisions collected by the ATLAS detector at energies $\sqrt{s}$ =7, 8 TeV
- B^0 production asymmetry measured in $B_d \to J/\psi K^{*0}$:

$$A_P = (+0.25 \pm 0.48 \pm 0.05) \times 10^{-2}$$

- $\Delta\Gamma_d/\Gamma_d$ extracted from the ratio (determined by MC) of reconstruction efficiencies of $B_d \to J/\psi K^{*0}$ and $B_d \to J/\psi K_S$ (comparing the decay time distributions)

$$\Delta\Gamma_d/\Gamma_d = (-0.1 \pm 1.1(\text{stat.}) \pm 0.9(\text{syst.}))\times 10^{-2}$$

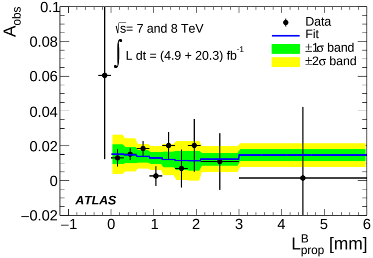

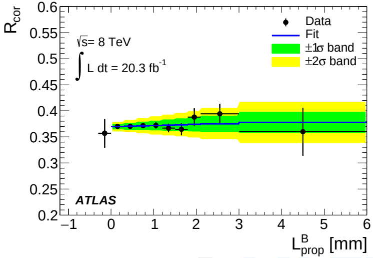

Systematic uncertainties

	ϕ_s [10^{-3} rad]	$\Delta\Gamma_s$ [10^{-3} ps^{-1}]	Γ_s [10^{-3} ps^{-1}]	$\|A_\parallel(0)\|^2$ [10^{-3}]	$\|A_0(0)\|^2$ [10^{-3}]	$\|A_S(0)\|^2$ [10^{-3}]	$\delta_\perp$ [10^{-3} rad]	$\delta_\parallel$ [10^{-3} rad]	$\delta_\perp - \delta_S$ [10^{-3} rad]
Tagging	19	0.4	0.3	0.2	0.2	1.1	17	19	2.3
ID alignment	0.8	0.2	0.5	< 0.1	< 0.1	< 0.1	11	7.2	< 0.1
Acceptance	0.5	0.3	< 0.1	1.0	0.9	2.9	37	64	8.6
Time efficiency	0.2	0.2	0.5	< 0.1	< 0.1	0.1	3.0	5.7	0.5
Best candidate selection	0.4	1.6	1.3	0.1	1.0	0.5	2.3	7.0	7.4
Background angles model:									
Choice of fit function	2.5	< 0.1	0.3	1.1	< 0.1	0.6	12	0.9	1.1
Choice of p_T bins	1.3	0.5	< 0.1	0.4	0.5	1.2	1.5	7.2	1.0
Choice of mass window	9.3	3.3	< 0.1	0.4	0.8	0.4	17	8.6	1.8
Choice of sidebands intervals	0.4	0.1	0.1	0.3	0.3	1.3	4.4	7.4	2.3
Dedicated backgrounds:									
B_d^0	2.6	1.1	< 0.1	0.2	3.1	1.5	10	23	2.1
Λ_b	1.6	0.3	0.2	0.5	1.2	1.8	14	30	0.8
Alternate Δm_s	1.0	< 0.1	< 0.1	< 0.1	< 0.1	< 0.1	15	4.0	< 0.1
Fit model:									
Time res. sig frac	1.4	1.1	0.5	0.5	0.6	0.8	12	30	0.4
Time res. p_T bins	0.7	0.5	0.8	0.1	0.1	0.1	2.2	14	0.7
S-wave phase	0.3	< 0.1	< 0.1	< 0.1	< 0.1	0.2	8.0	15	37
Fit bias	5.7	1.3	1.2	1.3	0.4	1.1	3.3	19	0.3
Total	22	4.3	2.2	2.3	3.8	4.6	55	88	39

ATLAS EXPERIMENT

Systematic uncertainties

Solution a:

	$\Delta\Gamma$	Γ_s	$\lvert A_{\|\|}(0)\rvert^2$	$\lvert A_0(0)\rvert^2$	$\lvert A_S(0)\rvert^2$	$\delta_{\|\|}$	$\delta_\perp$	$\delta_\perp - \delta_S$
ϕ_s	−0.080	0.017	−0.003	−0.004	−0.007	0.007	0.004	−0.007
$\Delta\Gamma$	1	−0.586	0.090	0.095	0.051	0.032	0.005	0.020
Γ_s		1	−0.125	−0.045	0.080	−0.086	−0.023	0.015
$\lvert A_{\|\|}(0)\rvert^2$			1	−0.341	−0.172	0.522	0.133	−0.052
$\lvert A_0(0)\rvert^2$				1	0.276	−0.103	−0.034	0.070
$\lvert A_S(0)\rvert^2$					1	−0.362	−0.118	0.244
$\delta_{\|\|}$						1	0.254	−0.085
$\delta_\perp$							1	0.001

Solution b:

	$\Delta\Gamma$	Γ_s	$\lvert A_{\|\|}(0)\rvert^2$	$\lvert A_0(0)\rvert^2$	$\lvert A_S(0)\rvert^2$	$\delta_{\|\|}$	$\delta_\perp$	$\delta_\perp - \delta_S$
ϕ_s	−0.084	0.019	−0.011	−0.003	−0.006	0.007	0.005	−0.006
$\Delta\Gamma$	1	−0.586	0.090	0.096	0.057	−0.029	−0.010	0.021
Γ_s		1	−0.116	−0.048	0.071	0.070	0.017	0.015
$\lvert A_{\|\|}(0)\rvert^2$			1	−0.338	−0.110	−0.444	−0.106	−0.052
$\lvert A_0(0)\rvert^2$				1	0.269	0.080	0.017	0.070
$\lvert A_S(0)\rvert^2$					1	0.291	0.060	0.251
$\delta_{\|\|}$						1	0.235	0.097
$\delta_\perp$							1	0.056

CP Violation Measurement: Angular analysis

k	$\mathcal{O}^{(k)}(t)$ — $\pm \rightarrow B_s/\bar{B}_s$	$g^{(k)}(\theta_T,\psi_T,\phi_T)$
1	$\frac{1}{2}\lvert A_0(0)\rvert^2 \left[(1+\cos\phi_s)\, e^{-\Gamma_{\mathrm{L}}^{(s)}t} + (1-\cos\phi_s)\, e^{-\Gamma_{\mathrm{H}}^{(s)}t} \pm 2e^{-\Gamma_s t}\sin(\Delta m_s t)\sin\phi_s\right]$	$2\cos^2\psi_T(1-\sin^2\theta_T\cos^2\phi_T)$
2	$\frac{1}{2}\lvert A_\parallel(0)\rvert^2 \left[(1+\cos\phi_s)\, e^{-\Gamma_{\mathrm{L}}^{(s)}t} + (1-\cos\phi_s)\, e^{-\Gamma_{\mathrm{H}}^{(s)}t} \pm 2e^{-\Gamma_s t}\sin(\Delta m_s t)\sin\phi_s\right]$	$\sin^2\psi_T(1-\sin^2\theta_T\sin^2\phi_T)$
3	$\frac{1}{2}\lvert A_\perp(0)\rvert^2 \left[(1-\cos\phi_s)\, e^{-\Gamma_{\mathrm{L}}^{(s)}t} + (1+\cos\phi_s)\, e^{-\Gamma_{\mathrm{H}}^{(s)}t} \mp 2e^{-\Gamma_s t}\sin(\Delta m_s t)\sin\phi_s\right]$	$\sin^2\psi_T\sin^2\theta_T$
4	$\frac{1}{2}\lvert A_0(0)\rvert\lvert A_\parallel(0)\rvert\cos\delta_\parallel$ $\left[(1+\cos\phi_s)\, e^{-\Gamma_{\mathrm{L}}^{(s)}t} + (1-\cos\phi_s)\, e^{-\Gamma_{\mathrm{H}}^{(s)}t} \pm 2e^{-\Gamma_s t}\sin(\Delta m_s t)\sin\phi_s\right]$	$-\frac{1}{\sqrt{2}}\sin 2\psi_T\sin^2\theta_T\sin 2\phi_T$
5	$\lvert A_\parallel(0)\rvert\lvert A_\perp(0)\rvert[\frac{1}{2}(e^{-\Gamma_{\mathrm{L}}^{(s)}t} - e^{-\Gamma_{\mathrm{H}}^{(s)}t})\cos(\delta_\perp-\delta_\parallel)\sin\phi_s$ $\pm e^{-\Gamma_s t}(\sin(\delta_\perp-\delta_\parallel)\cos(\Delta m_s t) - \cos(\delta_\perp-\delta_\parallel)\cos\phi_s\sin(\Delta m_s t))]$	$\sin^2\psi_T\sin 2\theta_T\sin\phi_T$
6	$\lvert A_0(0)\rvert\lvert A_\perp(0)\rvert[\frac{1}{2}(e^{-\Gamma_{\mathrm{L}}^{(s)}t} - e^{-\Gamma_{\mathrm{H}}^{(s)}t})\cos\delta_\perp\sin\phi_s$ $\pm e^{-\Gamma_s t}(\sin\delta_\perp\cos(\Delta m_s t) - \cos\delta_\perp\cos\phi_s\sin(\Delta m_s t))]$	$\frac{1}{\sqrt{2}}\sin 2\psi_T\sin 2\theta_T\cos\phi_T$
7	$\frac{1}{2}\lvert A_S(0)\rvert^2 \left[(1-\cos\phi_s)\, e^{-\Gamma_{\mathrm{L}}^{(s)}t} + (1+\cos\phi_s)\, e^{-\Gamma_{\mathrm{H}}^{(s)}t} \mp 2e^{-\Gamma_s t}\sin(\Delta m_s t)\sin\phi_s\right]$	$\frac{2}{3}\left(1-\sin^2\theta_T\cos^2\phi_T\right)$
8	$\lvert A_S(0)\rvert\lvert A_\parallel(0)\rvert[\frac{1}{2}(e^{-\Gamma_{\mathrm{L}}^{(s)}t} - e^{-\Gamma_{\mathrm{H}}^{(s)}t})\sin(\delta_\parallel-\delta_S)\sin\phi_s$ $\pm e^{-\Gamma_s t}(\cos(\delta_\parallel-\delta_S)\cos(\Delta m_s t) - \sin(\delta_\parallel-\delta_S)\cos\phi_s\sin(\Delta m_s t))]$	$\frac{1}{3}\sqrt{6}\sin\psi_T\sin^2\theta_T\sin 2\phi_T$
9	$\frac{1}{2}\lvert A_S(0)\rvert\lvert A_\perp(0)\rvert\sin(\delta_\perp-\delta_S)$ $\left[(1-\cos\phi_s)\, e^{-\Gamma_{\mathrm{L}}^{(s)}t} + (1+\cos\phi_s)\, e^{-\Gamma_{\mathrm{H}}^{(s)}t} \mp 2e^{-\Gamma_s t}\sin(\Delta m_s t)\sin\phi_s\right]$	$\frac{1}{3}\sqrt{6}\sin\psi_T\sin 2\theta_T\cos\phi_T$
10	$\lvert A_0(0)\rvert\lvert A_S(0)\rvert[\frac{1}{2}(e^{-\Gamma_{\mathrm{H}}^{(s)}t} - e^{-\Gamma_{\mathrm{L}}^{(s)}t})\sin\delta_S\sin\phi_s$ $\pm e^{-\Gamma_s t}(\cos\delta_S\cos(\Delta m_s t) + \sin\delta_S\cos\phi_s\sin(\Delta m_s t))]$	$\frac{4}{3}\sqrt{3}\cos\psi_T\left(1-\sin^2\theta_T\cos^2\phi_T\right)$

CP Violation Measurement: Using Tag Information in B_s^0 Fit

- Opposite side lepton or jet, with tracks in cone $\Delta R < 0.5$

$$Q = \frac{\sum_i^{Ntracks} q^i (p_{\mathrm{T}}^i)^\kappa}{\sum_i^{Ntracks} (p_{\mathrm{T}}^i)^\kappa}$$

- Events separated - discrete contribution (cone charge +1 or -1) and continuous contribution
- By using calibration curves: we get the B_s^0 tag probability
- Fractions of events f_{+1} and f_{-1} with charges +1 and -1, respectively, are determined separately for signal and background
- Remaining fraction of events, $1 - f_{+1} - f_{-1}$, constitute the continuous part

Tag Method	Signal		Background	
	f_{+1}	f_{-1}	f_{+1}	f_{-1}
Tight μ	0.073 ± 0.005	0.081 ± 0.006	0.051 ± 0.001	0.053 ± 0.001
Medium e	0.18 ± 0.01	0.16 ± 0.01	0.159 ± 0.003	0.161 ± 0.003
Low-pt μ	0.120 ± 0.008	0.125 ± 0.008	0.074 ± 0.001	0.080 ± 0.001
Jets	0.038 ± 0.002	0.039 ± 0.002	0.0324 ± 0.0004	0.0323 ± 0.0004

CP Violation Measurement: Using Tag Information in B_s^0 Fit

- Opposite side lepton or jet, with tracks in cone $\Delta R < 0.5$

$$Q = \frac{\sum_i^{Ntracks} q^i (p_{\mathrm{T}}^i)^\kappa}{\sum_i^{Ntracks} (p_{\mathrm{T}}^i)^\kappa}$$

- Events separated - discrete contribution (cone charge +1 or -1) and continuous contribution
- By using calibration curves: we get the B_s^0 tag probability
- Fractions of events f_{+1} and f_{-1} with charges +1 and -1, respectively, are determined separately for signal and background
- Remaining fraction of events, $1 - f_{+1} - f_{-1}$, constitute the continuous part

Tag method	Signal	Background
Tight μ	0.0400 ± 0.0006	0.0316 ± 0.0001
Electron	0.0187 ± 0.0004	0.01480 ± 0.0001
Low-pT μ	0.0291 ± 0.0005	0.0264 ± 0.0001
Jets	0.144 ± 0.001	0.1196 ± 0.0002
Untagged	0.767 ± 0.003	0.8077 ± 0.0005

CP Violation Measurement: Tagging